On infiltration and infiltration characteristic times

Mehdi Rahmati[1,2], Borja Latorre[3], David Moret-Fernández[3], Laurent Lassabatere[4], Nima Talebian[5], Dane Miller[5], Renato Morbidelli[6], Massimo Iovino[7], Vincenzo Bagarello[7], Mohammad Reza Neyshabouri[8], Ying Zhao[9], Jan Vanderborght[2], Lutz Weihermüller[2], Rafael Angulo Jaramillo[4], Dani Or[10, 11], Martinus Th. van Genuchten[12, 13], Harry Vereecken[2]

[1]Department of Soil Science and Engineering, Faculty of Agriculture, University of Maragheh, Maragheh, Iran

[2]Forschungszentrum Jülich GmbH, Institute of Bio- and Geosciences: Agrosphere (IBG-3), Jülich, Germany

[3]Departamento de Suelo y Agua, Estación Experimental de Aula Dei, Consejo Superior de Investigaciones Científicas (CSIC), PO Box 13034, 50080 Zaragoza, Spain

[4]Univ Lyon, Université Claude Bernard Lyon 1, CNRS, ENTPE, UMR5023 LEHNA, F-69518, Vaulx-en-Velin, France

[5]Faculty of Society & Design, Bond University, Robina QLD 4226, Australia

[6]Department of Civil and Environmental Engineering, University of Perugia, Perugia, Italy

[7]Department of Agricultural, Food and Forest Sciences, University of Palermo, Italy

[8]Department of Soil Science and Engineering, Faculty of Agriculture, University of Tabriz, Tabriz, Iran

[9]College of Resources and Environmental Engineering, Ludong University, Yantai 264025, China

[10]Department of Environmental Systems Science, ETH Zurich, Switzerland

[11]Division of Hydrologic Sciences (DHS) - Desert Research Institute, Reno, NV, USA

[12]Department of Earth Sciences, Utrecht University, Utrecht, Netherlands.

[13]Center for Environmental Studies, CEA, São Paulo State University Rio Claro, Brazil

Corresponding author: Mehdi Rahmati (mehdirmti@gmail.com, m.rahmati@fz-juelich.de)

ORCID: https://orcid.org/0000-0001-5547-6442

Key points

- A new formulation for infiltration characteristic time, t_{grav}, is provided.

- The reformulated t_{grav} seems to be a better criterion for convergence time of Philip's truncated infiltration equations.
- The usage of reformulated t_{grav} improves predictions of soil hydraulic parameters.

Abstract

In his seminal paper on solution of the infiltration equation, Philip (1957) proposed a gravity time, t_{grav}, to estimate practical convergence time of his infinite time series expansion, TSE. The parameter t_{grav} refers to a point in time where infiltration is dominated equally by capillarity and gravity derived from the first two (dominant) terms of the TSE expansion. Evidence suggests that the applicability of the truncated two-term equation of Philip has time limit requiring higher order TSE terms to better describe the infiltration process for times exceeding that limit. Since the conceptual definition of t_{grav} is valid regardless of the infiltration model used, we opted to reformulate t_{grav} using the analytic approximation proposed by Parlange et al. (1982) valid for all times. In addition to the roles of soil sorptivity (S) and saturated (K_{s}) and initial (K_{i}) hydraulic conductivities, we explored effects of a soil specific shape parameter on the behavior of t_{grav}. We show that the reformulated t_{grav} (notably $t_{\text{grav}} = F(\beta)\frac{S^2}{(K_s-K_i)^2}$, where $F(\ )$ is a -dependent function) is about 3 times larger than the classical t_{grav} given by $t_{grav,\ \text{Philip}} = \frac{S^2}{(K_s-K_i)^2}$. The differences between original $t_{\text{grav, Philip}}$ and the revised t_{grav} increase for fine textured soils thus affecting the time needed to attain steady-state infiltration and the use of infiltration for inferring soil hydraulic properties. Results show that the proposed t_{grav} is a better indicator for convergence time than $t_{\text{grav, Philip}}$. For attainment of the steady-state infiltration, both time parameters are suitable for coarse-textured soils, but not for fine-textured soils for which t_{grav} is too conservative and $t_{\text{grav, Philip}}$ too short. Using t_{grav} will improve predictions of the soil hydraulic parameters (particularly K_{s}) from infiltration data as compared to $t_{\text{grav, Philip}}$.

Keywords: Convergence time, Hydraulic conductivity, Infiltration, Sorptivity, Steady state

Introduction

Infiltration is a key hydrological process in the partitioning rainfall reaching the land surface into water entering the soil profile and the portion that ponds and runoffs. Infiltration and runoff trigger various secondary processes including erosion (e.g., Assouline and Ben-Hur, 2006; Garrote and Bras, 1995; Poesen and Valentin, 2003), changes in stream flow and flooding events (e.g., Garrote and Bras, 1995), landslides and debris flows on hillslopes (e.g., Iverson, 2000; Lehmann and Or, 2012), water available to vegetation (e.g., Verhoef and Egea, 2013) and affect exchange of water and energy between the soil and atmosphere

(Kim et al., 2017; MacDonald et al., 2018). Knowledge about infiltration is of high relevance for various scientific disciplines. A recent comprehensive review of Vereecken et al. (2019) highlights the importance of infiltration processes at scales ranging from the Pedon to global.

In general, the infiltration process can be described by solving the Richards (1931) equation when the relationships between soil water content, matrix potential, and hydraulic conductivity are defined explicitly. Alternatively, direct measurement of actual infiltration provides a convenient field approach to determine such soil hydraulic parameters as the sorptivity and the saturated hydraulic conductivity (Ross et al., 1996). Sorptivity (S) expresses the capacity of a soil to absorb and release water by capillarity, while the saturated hydraulic conductivity (K_{s}) reflects the ability of a soil to transmit water under the influence of gravity.

The time series expansion (TSE) introduced by Philip (1957), as a unique solution of the Richards equation, remains a widely used model for 1D ponded infiltration. Although, the TSE comprises an infinite series of different components, generally only the first two terms are being used in practice, with the higher-order terms in the infinite time series (as well as the sum and convergence criteria, a given time that the $I(t)$ function converges to the measured infiltration curve for all time shorter than that) requiring a more systematic analysis. In order to analyze the convergence of the TSE, Philip (1957) introduced a characteristic time termed gravity time, t_{grav}, at which gravity begins to dominate infiltration over capillarity. Philip (1957) assumed t_{grav} to be a practical measure for the time range of useful convergence of the TSE. Hereby, t_{grav} was simply formulated in terms of S and $\Delta K = K_{\mathrm{s}}$ - K_{i}, where K_{i} is the hydraulic conductivity at the initial (prior the infiltration) soil water content, $_{\mathrm{i}}$. Although not mentioned explicitly by Philip (1957), one may infer that only two first terms of the TSE are used to formulate t_{grav}. The definition of t_{grav} is then explicit since the first term of the infiltration equation represents the effects of capillarity, and the second term the effects of gravity.

Beside the question that whether t_{grav} is a correct indicator for convergence time of Philip's TSE and its truncated forms, a precise determination of t_{grav} itself is of great importance. A limitation of the two-term infiltration approximation, as used to formulate the t_{grav}, is that it cannot be used for long infiltration times. Several studies indicate that the higher-order TSE terms can describe the infiltration process much better the two-term equation in some soils (Kutílek and Krejca, 1987; Rahmati et al., 2019; 2020). On the other hand, conceptually, t_{grav} that marks when 50% of the cumulative infiltration is dominated by capillarity offers a generalizable alternative concept in the sense that it is valid regardless of the number of terms included in the infiltration equation as well as regardless of the used model. A possible improvement when reformulating t_{grav} could be usage of an infiltration model without any time constraints. An attractive approach for this is the analytic approximation provided by Parlange et al.

(1982)[1] and which we will refer to as AAP in the subsequent. This is because their formulation is 1) widely adopted due to its physical basis; 2) valid for the entire infiltration process (Haverkamp et al., 1994; Parlange et al., 1982); and 3) closely approximates the complete TSE expansion (Moret-Fernández et al., 2020; Rahmati et al., 2019; 2020), thus enabling users to determine which component reflects the capillary or gravity effects on infiltration (Rahmati et al., 2020). In addition to S and ΔK, the AAP formulation includes a soil specific shape parameter that also impacts infiltration. Therefore, we seek to broaden the formulation of t_{grav} by considering all three variables S, ΔK, and as used in the AAP formulation so that the general features of the cumulative infiltration curve can be captured for different soils.

Adding terms to the TSE based t_{grav} formulation reflects the persistent effects of capillarity at relatively long infiltration times where the infiltration is dominated by gravity. If the two-term TSE infiltration equation is used, the first term is purely capillary driven and the second term driven by gravity (Lassabatere et al., 2006; Philip and Farrell, 1964, among others). However, the role of higher-order TSE terms, whether capillary- or gravity-driven, remains controversial, primarily because they contain ratios of ${K_s}^{n\text{-}1}/S^{n\text{-}2}$ (with $n = 1, 2, ..., \infty$). For example, Rahmati et al. (2020, 2021) analyzed the contributions of the higher order TSE terms under the premise that the role of gravity increases with increasing infiltration time. They concluded that although the higher-order terms still include the capillary parameter S, the terms remain largely controlled by gravity. A characteristic of the TSE is that all higher terms (those beyond the first two) have negligible impact on the onset of infiltration, whereas their contribution increases with increasing infiltration time. Since S is a capillary parameter, an important question arises about the role of S in the higher order TSE terms, and whether these terms mainly reflect gravity. A simple answer to this question can be found in the mathematical form of the infinite series in terms of as derived by Philip (1957). The series contains the variables S and K_{s} for all infiltration times, but with significantly diminishing contributions of S beyond the first (absorption) term. Also, Philip's solution of the Richards (1931) equation involves a perturbation of the exact absorption case without gravity, while also considering uniform soil properties and initial soil water content. These premises are often violated since the advancing infiltration front may reach layers with different water retention and hydraulic conductivities, thereby affecting physically and mathematically the infiltration rate at the surface. From a physical perspective, gravity will dominate the flow at late infiltration times, and hence one may expect then vertically downward gravity-driven saturated flow (Waechter and Philip, 1985). However, by neglecting capillary, no information on the transition from near-dryness to near-saturation in regions below the in-

[1] [] - The analytic approximation of Parlange et al. (1982) has been referred to as "quasi-exact implicit formulation of Haverkamp et al. (1994)" by several authors. While Haverkamp et al. (1994) have introduced useful refinements to the original expression of Parlange et al. (1982), in line with scientific convention, the expression (and modification thereof) should be referred to as the Parlange et al. (1982) equation, like the attribution made by Haverkamp et al. (1994).

filtration front will be obtained. As correctly stated by Waechter and Philip (1985), this is a "physically interesting and practically important limit of flows strongly dominated by gravity, with capillary effects weak but nonzero".

Because of the above ambiguities in the expression of t_{grav}, this study aims to clarify the definition of the characteristic infiltration time. Specific objectives are: 1) to reformulate the infiltration characteristic time t_{grav} using the AAP formulation (Parlange et al., 1982), 2) to study its relation to the classical t_{grav} introduced by Philip (1957), hereafter denoted as $t_{\text{grav, Philip}}$, and 3) to discuss potential applications of this soil property.

1.

Theoretical Development

(a)

Philip's infiltration theory

Based on an exact solution of the Richards (1931) equation, Philip (1957) derived the following expression for the 1D ponded infiltration rate, known as Philip's time series expansion (TSE):

$$I(t) = A_1 t^{\frac{1}{2}} + (A_2 + K_i)\, t + \sum_{n=3}^{\infty} A_n t^{\frac{n}{2}} \quad (1)$$

where I(t) denote the cumulative infiltration [L] at a given time t [T] and A_1 to A_∞ [L/T$^{n/2}$] are coefficients of the infinite time series:

$$A_n \geq \frac{K_s^{n-1}}{S^{n-2}}, \quad n = 1, 2, \ \ldots, \ \infty \quad (2)$$

Philip (1957) showed that A_1 is equal to the sorptivity S, while A_2 is proportional to K_{s}, suggesting that $A_2 = cK_s$, where c is a constant equal to $^1/_2$, $^2/_3$, and 0.38 depending upon the selected model (i.e., linearized, -function, and/or nonlinear).

Philip (1957) also determined the time domain validity of his TSE formulation. By comparing the time and geometric series equations, he found that the series solution should converge to the measured infiltration curve for $t < \left(\frac{S}{A_2}\right)^2$. After noting that in most cases $K_{\text{i}}/K_{\text{s}} \ll 1$ and $A_2 \approx \frac{1}{2}(K_s - K_i)$, Philip (1957) concluded that the convergence time could be defined as $t < 4t_{\text{grav, Philip}}$. Using S, K_{s}, and K_{i}, he approximated $t_{\text{grav,Philip}}$ as:

$$t_{grav,\ Philip} = \left(\frac{S}{K_s - K_i}\right)^2 \quad (3)$$

For initially dry soil conditions such that K_i can be neglected, the above equation simplifies to:

$$t_{grav,\ Philip} = \left(\frac{S}{K_s}\right)^2 \quad (4)$$

Philip (1957) furthermore showed that the condition $t < 4t_{\text{grav, Philip}}$ was too conservative and that the factor 4 could be replaced by a smaller value. Nominally, $t \leq t_{\text{grav, Philip}}$ expresses the practical convergence time for the TSE. Similarly as Eq. (4), Philip and Farrell (1964) defined the infiltration characteristic length, $I_{\text{grav, Philip}}$, as:

$$I_{grav,\ Philip} = \frac{S^2}{K_s - K_i} \overset{K_i \approx 0}{\rightarrow} I_{grav,\ \ Philip} = \frac{S^2}{K_s} \quad (5)$$

Parlange's analytical solution of the infiltration equation

Equation (3) holds subject to the approximate time constraint that an attractive approach to overcome the time constraint is through comparisons with AAP. The APP solution, which is valid for all times and gives an accurate estimate of the cumulative infiltration, can be expanded also in three-term (3T) or higher approximations, from which a more reliable estimate of t_{grav} can be derived. We first provide the background of the AAP as summarized by Rahmati et al. (2020).

The AAP cumulative infiltration solution (Parlange et al., 1982) which is redefined by Haverkamp et al. (1994) is given by:

$$\frac{2\,K^2}{S^2}t = \frac{2}{1-\beta}\frac{K(I-K_i t)}{S^2} - \frac{1}{1-\beta}\ln\left[\frac{1}{\beta}\exp\left\{\frac{2\beta\,K(I-K_i t)}{S^2}\right\} + \frac{\beta-1}{\beta}\right] \quad (6)$$

where is a soil-dependent dimensionless integral shape parameter, usually fixed at 0.6 (default value). Fuentes et al. (1992) demonstrated that the shape parameter is related to the soil hydraulic functions by:

$$\beta = 2 - 2^{\frac{\int_{\theta_i}^{\theta_s}\left(\frac{K-K_i}{K_s-K_i}\right)\left(\frac{\theta_s-\theta_i}{\theta-\theta_i}\right)D(\theta)\mathrm{d}}{\int_{\theta_i}^{\theta_s}D(\theta)\mathrm{d}}} \quad (7)$$

where $_s$ is the saturated volumetric water content (L^3L^{-3}), $_i$ is the initial water content (L^3L^{-3}), and $D(\ )$ is the soil water diffusivity. For initially dry soils (with $K_i \sim 0$), the AAP solution reduces to:

$$\frac{2K_s^2}{S^2}t = \frac{2}{1-\beta}\frac{K_s}{S^2}I - \frac{1}{1-\beta}\ln\left[\frac{1}{\beta}\exp\left(\frac{2\beta K_s}{S^2}I\right) + \frac{\beta-1}{\beta}\right] \quad (8)$$

A simplified two-term (2T) approximate expansion of the Eq. (8) was proposed by Haverkamp et al. (1994) to describe the transient state valid for short to intermediate infiltration times. The expansion is identical to Philip (1957) two-term equation:

$$I(t) = c(1)t^{\frac{1}{2}} + c(2)t \quad (9)$$

where

$$c(1) = S \quad (10)$$
$$c(2) = \frac{2-\beta}{3}K_s$$

Additional expansions were proposed by Rahmati et al. (2019) using three terms (3T), by Moret-Fernández et al. (2020) considering four terms (4T), and Rahmati et al. (2020) using five terms (5T), i.e.,

$$I(t) = c(1)t^{\frac{1}{2}} + c(2)t + c(3)t^{\frac{3}{2}} \quad (11)$$
$$I(t) = c(1)t^{\frac{1}{2}} + c(2)t + c(3)t^{\frac{3}{2}} + c(4)t^2 \quad (12)$$
$$I(t) = c(1)t^{\frac{1}{2}} + c(2)t + c(3)t^{\frac{3}{2}} + c(4)t^2 + c(5)t^{\frac{5}{2}} \quad (13)$$

where c(3) to c(5) are defined as:

$$c(3) = \frac{1}{9}\left(\beta^2 - \beta + 1\right)\frac{K_s^2}{S}$$
$$c(4) = \frac{2}{135}(\beta-2)(\beta+1)(1-2\beta)\frac{K_s^3}{S^2} \quad (14)$$
$$c(5) = \frac{1}{270}\left(\beta^2 - \beta + 1\right)^2\frac{K_s^4}{S^3}$$

Exact implicit formulation of the characteristic time $t_{\mathbf{grav}}$

According to the basic definition of t_{grav}, one can rewrite the TSE (Eq. 1) at time equal to t_{grav} (Rahmati et al., 2020) as:

$$\frac{1}{2} I_{\text{grav}} = S t_{\text{grav}}^{\frac{1}{2}} \quad (15)$$

where I_{grav} is the cumulative infiltration at time t_{grav}, also known as the infiltration characteristic length. I_{grav} in Eq. (15) can be computed immediately by evaluating Eq. (1) at time t_{grav}. Since Philip's TSE is not clearly defined when using a limited number of terms, we consider it more robust to reformulate t_{grav} by making use of AAP solution, which is valid for entire infiltration time. To do this, Eq. (6) is redefined in terms of $t = t_{\text{grav}}$ by substituting I_{grav} from Eq. (15) into Eq. (6) to give:

$$\frac{2\,K^2}{S^2} t_{\text{grav}} = \frac{2}{1-\beta} \frac{K\left(2St_{\text{grav}}^{\frac{1}{2}} - K_i t_{\text{grav}}\right)}{S^2} - \frac{1}{1-\beta} \ln\left[\frac{1}{\beta} \exp\left\{\frac{2\beta\, K\left(2St_{\text{grav}}^{\frac{1}{2}} - K_i t_{\text{grav}}\right)}{S^2}\right\} + \frac{\beta-1}{\beta}\right] \quad (16)$$

Assuming that K_{s}, S, K_{i}, and are known, this equation can be solved analytically for t_{grav} using MATLAB, Mathematica, Python, or some other software package. An alternative is to use the definition of the characteristic time (Eq. 15) where capillary and gravity have the same effect on infiltration. Values of t_{grav} can be then determined easily immediately by numerically computing I_{AP} and finding the root of the equation:

$$I_{\text{AAP}}(t_{\text{grav}}) - 2St_{\text{grav}}^{1/2} = 0 \quad (17)$$

As an alternative, a computationally more effective scaling procedure as proposed by Varado et al. (2006) and further developed by Lassabatere et al. (2009) can be used. For this purpose, we scale the cumulative infiltration, $I(t)$, and time, t, by:

$$I(t) = \frac{S^2}{2\,K} I^*\left(t^*\right) + K_i \mathrm{t} \quad (18)$$
$$t = \frac{S^2}{2\,K^2} t^*$$

Rewriting the above equations for $t = t_{\text{grav}}$ yields:

$$I\left(t_{\text{grav}}\right) = \frac{S^2}{2\,K} I^*\left(t_{\text{grav}}^*\right) + \frac{S^2 K_i}{2\,K^2} t_{\text{grav}}^* \quad (19)$$
$$t_{\text{grav}} = \frac{S^2}{2\,K^2} t_{\text{grav}}^*$$

where t_{grav}^* is the scaled t_{grav} parameters, and $I^*\left(t_{\text{grav}}^*\right)$ corresponds to the

scaled cumulative infiltration at t^*_{grav}. Substitution of the above expressions into Eq. (16) leads to:

$$t^*_{\text{grav}} = \frac{1}{1-\beta}\left(2\sqrt{2t^*_{\text{grav}}} - \frac{K_i}{K}t^*_{\text{grav}}\right) - \frac{1}{1-\beta}\ln\left[\frac{1}{\beta}\exp\left\{\beta\left(2\sqrt{2t^*_{\text{grav}}} - \frac{K_i}{K}t^*_{\text{grav}}\right)\right\} + \frac{\beta-1}{\beta}\right] \quad (20)$$

Several functions for the hydraulic conductivity could be used in Eq. (20). In this study we used the Mualem-van Genuchten (MvG) model (Mualem, 1976; van Genuchten, 1980) for K_i given by:

$$\frac{K(S_e)}{K_s} = S_e^{1/2}\left[1-\left(1-S_e^{1/m}\right)^m\right]^2, \qquad S_e = \frac{\theta-\theta_r}{\theta_s-\theta_r} \quad (21)$$

where $K(S_{\text{e}})$ is soil hydraulic conductivity at effective saturation (S_{e}), or alternatively at given soil water content , m is a model parameter, and $_{\text{s}}$ and $_{\text{r}}$ are the saturated and residual water contents (L^3 L^{-3}), respectively.

Substitution of Eq. (21) into Eq. (20) gives:

$$t^*_{\text{grav}} = \frac{1}{1-\beta}\left(2\sqrt{2t^*_{\text{grav}}} - \delta t^*_{\text{grav}}\right) - \frac{1}{1-\beta}\ln\left[\frac{1}{\beta}\exp\left\{\beta\left(2\sqrt{2t^*_{\text{grav}}} - \delta t^*_{\text{grav}}\right)\right\} + \frac{\beta-1}{\beta}\right] \quad (22)$$

where is a coefficient accounting for the effects of initial soil water content and the parameter m on t^*_{grav}:

$$\delta = \frac{S_{e,i}^{1/2}\left[1-\left(1-S_{e,i}^{1/m}\right)^m\right]^2}{1-S_{e,i}^{1/2}\left[1-\left(1-S_{e,i}^{1/m}\right)^m\right]^2}, \qquad 0 \leq \delta < 1 \quad (23)$$

Equation (22) is identical to Eq. (16), except that K_{s}, K_{i}, and S are eliminated to lead to a more generalized definition of from where we can view as a function of the infiltration-related soil variable and the functional coefficient given by:

$$t^*_{\text{grav}} = c(\beta, \delta) \quad (24)$$

The function $c(\ ,\ )$ is to be obtained from Eq. (22) by numerical resolution using a root-finding algorithm. Finally, the dimensional t_{grav} can be recovered immediately from Eq. (18) to yield:

$$t_{\mathrm{grav}} = F(\beta,\delta)\left(\frac{S}{K}\right)^2 \quad (25)$$

where $F(\ ,\ )$ defines a functional relationship depending on and :

$$F(\beta,\delta) = \frac{c(\beta,\delta)}{2} \quad (26)$$

For an initially dry soil ($\lim_{S_{e,i}\to 0}\delta = 0$), one can simply set $= 0$. Eq. (22) then simplifies to:

$$t^*_{\mathrm{grav}} = \frac{1}{1-\beta}\left(2\sqrt{2t^*_{\mathrm{grav}}} - ln\left[\frac{1}{\beta}\exp\left\{2\beta\sqrt{2t^*_{\mathrm{grav}}}\right\} + \frac{\beta-1}{\beta}\right]\right) \quad (27)$$

In this case, can be viewed as a function of only. Eq. (25) can then be simplified also by setting $K_{\mathrm{i}} = 0$:

$$t_{\mathrm{grav}} = F(\beta,\delta=0)\left(\frac{S}{K_s}\right)^2 = F(\beta)\left(\frac{S}{K_s}\right)^2 \quad (28)$$

By having t_{grav} reformulated, one can simply use Eq. (15) to compute the infiltration characteristic length by:

$$I_{\mathrm{grav}} = 2\sqrt{F(\beta,\delta)}\frac{S^2}{K} \quad \overset{\mathrm{K_i}\approx\ 0}{\rightarrow} \quad I_{\mathrm{grav}} = 2\sqrt{F(\beta)}\frac{S^2}{K_s} \quad (29)$$

Approximate explicit expression of the characteristic time t_{grav}

Although formally it is possible to numerically evaluate the functional relationship $F(\ )$, the equation might be too impractical for many applications. We use, therefore, alternatively the 3T approximation to obtain an explicit formulation for $F(\ )$ and consequently for t_{grav}. Calculating I_{grav} at time t_{grav} using the 3T approximation (Eq. 11), and substituting it in Eq. (15), yields:

$$S = \frac{1}{2}\frac{St_{\mathrm{grav}}^{\frac{1}{2}} + \frac{2-\beta}{3}K_s t_{\mathrm{grav}} + \frac{1}{9}(\beta^2-\beta+1)\frac{K_s^2}{S}t_{\mathrm{grav}}^{\frac{3}{2}}}{t_{\mathrm{grav}}^{\frac{1}{2}}} \quad (30)$$

In this expression, the initial value of the hydraulic conductivity, K_i, is neglected,

meaning that the expression should be considered only for initially dry soils. Simplifying and rearranging Eq. (30) results in a quadratic equation, where $\sqrt{t_{\text{grav}}}$ represents an unknown, and K_{s}, S, and represent knowns:

$$-S + \frac{2-\beta}{3} K_s t_{\text{grav}}^{\frac{1}{2}} + \frac{1}{9}(\beta^2 - \beta + 1)\frac{K_s^2}{S} t_{\text{grav}} = 0 \quad (31)$$

Solving Eq. (31) for $\sqrt{t_{\text{grav}}}$ in terms of its positive root results in the following expression:

$$F(\beta) = \left(\frac{3}{2} \frac{\sqrt{5\beta^2 - 8\beta + 8} - (2-\beta)}{(\beta^2 - \beta + 1)} \right)^2 \quad (32)$$

which shows that $F(\ )$ now explicitly depends on .

Test data for validation

The expressions above were obtained by using the AAP expansion. However, when evaluating their AAP based model, Parlange et al. (1982) made several assumptions that may not apply to real-world cases. Especially their proposed relation between and the hydraulic curves of the soil (see equation 6 in Haverkamp et al., 1994) seems problematic. For this reason we validated the proposed expressions of $F(\ )$ against synthetic infiltration data generated with the HYDRUS-1D software (Šimůnek et al., 2008, 2016). We used for this the hydraulic properties of 12 USDA soil textural classes (Table 1) as compiled by Carsel and Parrish (1988). The employed data are provided as supplemental material by Rahmati et al. (2020, 2021). Table 2 summarizes settings that were used for the HYDRUS-1D simulations. Readers are also referred to Rahmati et al. (2020, 2021) for details of the simulations.

Table 1. Soil hydraulic parameters of the van Genuchten (1980) (MvG) model for the soil water retention and hydraulic conductivity functions for 12 USDA textural classes as compiled by Carsel and Parrish (1988). The sorptivity (S) data were obtained from horizontal infiltration simulations by Rahmati et al. (2020). The MvG tortuosity parameter l for the hydraulic conductivity was fixed at 0.5 as used by van Genuchten (1980). Initial water contents $_{\text{i}}$ being modeled for initial water pressure head of 10000 cm were taken from Rahmati et al. (2020, 2021).

Parameters	$_{\text{r}}$	$_{\text{s}}$	$_{\text{i}}$		n	m	K_{s}	S	
	($\text{cm}^3\ \text{cm}^{-3}$)	(cm^{-1})			(cm h^{-1})	(cm $\text{h}^{-1/2}$)			
Clay	0.068	0.380	0.271	0.008	1.09	0.083	0.20	1.02	1.92
Clay loam	0.095	0.410	0.150	0.019	1.31	0.237	0.26	1.46	1.58

Parameters	r	s	i		n	m	K_s	S	
Loam	0.078	0.430	0.088	0.036	1.56	0.359	1.04	2.20	1.27
Loamy sand	0.057	0.410	0.057	0.124	2.28	0.561	14.6	6.22	0.80
Sand	0.045	0.430	0.045	0.145	2.68	0.627	29.7	9.23	0.60
Sandy clay	0.100	0.380	0.170	0.027	1.23	0.187	0.12	0.79	1.70
Sandy clay loam	0.100	0.390	0.111	0.059	1.48	0.324	1.31	1.61	1.36
Sandy loam	0.065	0.410	0.066	0.075	1.89	0.471	4.42	3.84	0.99
Silt	0.034	0.460	0.090	0.016	1.37	0.270	0.25	1.35	1.50
Silt loam	0.067	0.450	0.104	0.020	1.41	0.291	0.45	1.66	1.44
Silt clay	0.070	0.360	0.266	0.005	1.09	0.083	0.02	0.35	1.92
Silty clay loam	0.089	0.430	0.197	0.010	1.23	0.187	0.07	0.53	1.70

s, r, and i are the saturated, residual, and initial water contents; , n, and m are parameters of the van Genuchten (1980) soil hydraulic model; K_s is the saturated hydraulic conductivity; S is the soil sorptivity; is an infiltration constant defined by Parlange et al. (1982) and formulated by Fuentes et al. (1992).

Table 2. Parameters and conditions used for the HYDRUS-1D simulations to generate the synthetic infiltration data (adopted from Rahmati et al., 2020, 2021).

@ >p(- 2) * >p(- 2) * @ Simulation settings & Applied condition
Soil Profile depth & 200 cm
Upper boundary condition & Zero-pressure head
Lower boundary condition & Free drainage
Node Numbers for discretization & 401 non-equidistant (lower spacing to the top)
Simulation time & 24 hours
Internal interpolation tables & Disabled
Hydraulic model &

if $n > 1.2$

& MvG

if $n < 1.2$

& Modified MvG with an air-entry value of -2 cm

n is a parameter in the van Genuchten (1980), MvG, soil hydraulic functions.

Results and Discussion

Functional relationship of $F(\ ,\ )$ and t_{grav}

Figure 1 illustrates the variations of the functional $F(\ ,\ )$, as well as of t_{grav} (reformulated t_{grav} obtained for the AAP solution when 0) and $t_{grav,\ Philip}$ for the twelve USDA soil classes examined. Results indicate that t_{grav} varies between 15 minutes for sand and 996 hours for silty clay, with an average of 138 ± 80 hours over all soil classes. Excluding silty clay from the analysis, the range of t_{grav} gets narrower by varying between 15 minutes for sand and 183 hours for silty clay loam, with an average of 60 ± 19 hours. A clear trend can be detected with lower t_{grav} values for the coarser textures. This agrees with the physics of the flow processes involved in that lower soil capillary forces and higher flow rates are to be expected for the more coarse-textured soils with their larger pores.

Similarly to t_{grav}, Figure 1 shows that $F(\ ,\ )$ varies between 2.59 and 3.25, with the finer soil textural classes exhibiting higher $F(\ ,\ )$ values. These results indicate that the reformulated t_{grav} is approximately 2.59 to 3.25 times (with a mean value of 3.1) higher than $t_{grav,\ Philip}$, since $t_{grav} = F(\beta,\ \delta) \times t_{grav,\quad Philip}$. This probably also impacts the interpretation of infiltration data to be presented later in Section 3.5.

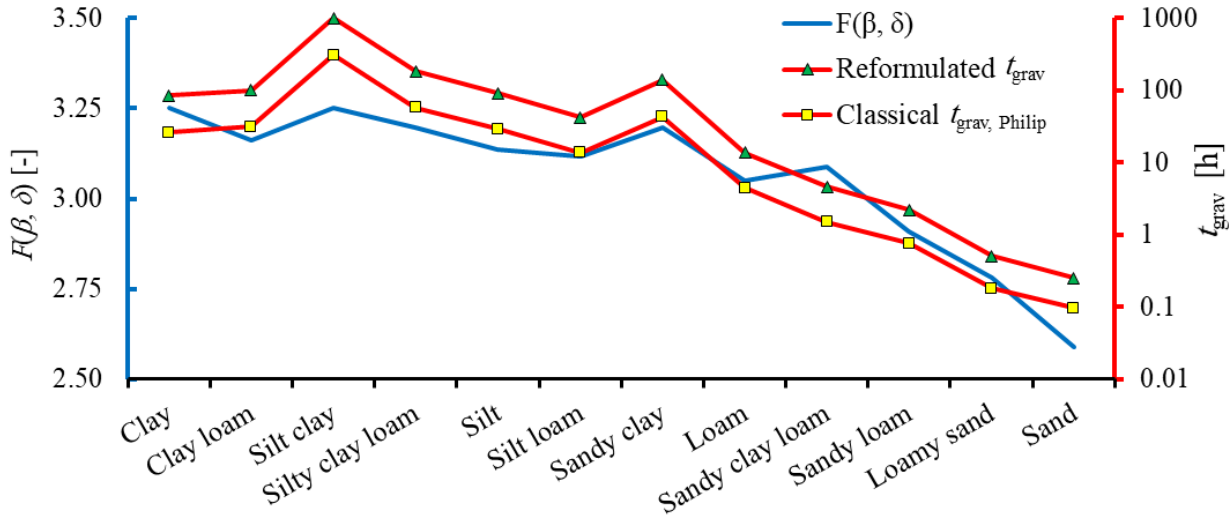

Figure 1. Variation in the functional relationship F(,) and reformulated and classical characteristic times (t_{grav} [h]) for the twelve USDA soil textural classes. Note that soils are ranked based on their texture and no function is defined for them.

Next, the relationships between $F(\ ,\ )$ versus and were analyzed. As can

be seen from the results in Fig. 2, $F(\ ,\ )$ increases linearly with $\ $, having a slope of 0.47 ($R^2 = 0.95$). On the other hand, $F(\ ,\ )$ increases nonlinearly with increasing $\ $, as expressed by a power law with an exponent of 0.011 ($R^2 = 0.50$). The curved line shows that changes in $\ $ near its lower bound have far greater effects on $F(\ ,\ )$ than at higher values when $\ > 0.1$. This is discussed in more detail next by also considering the dependency of $\ $ on m and $S_{e,i}$.

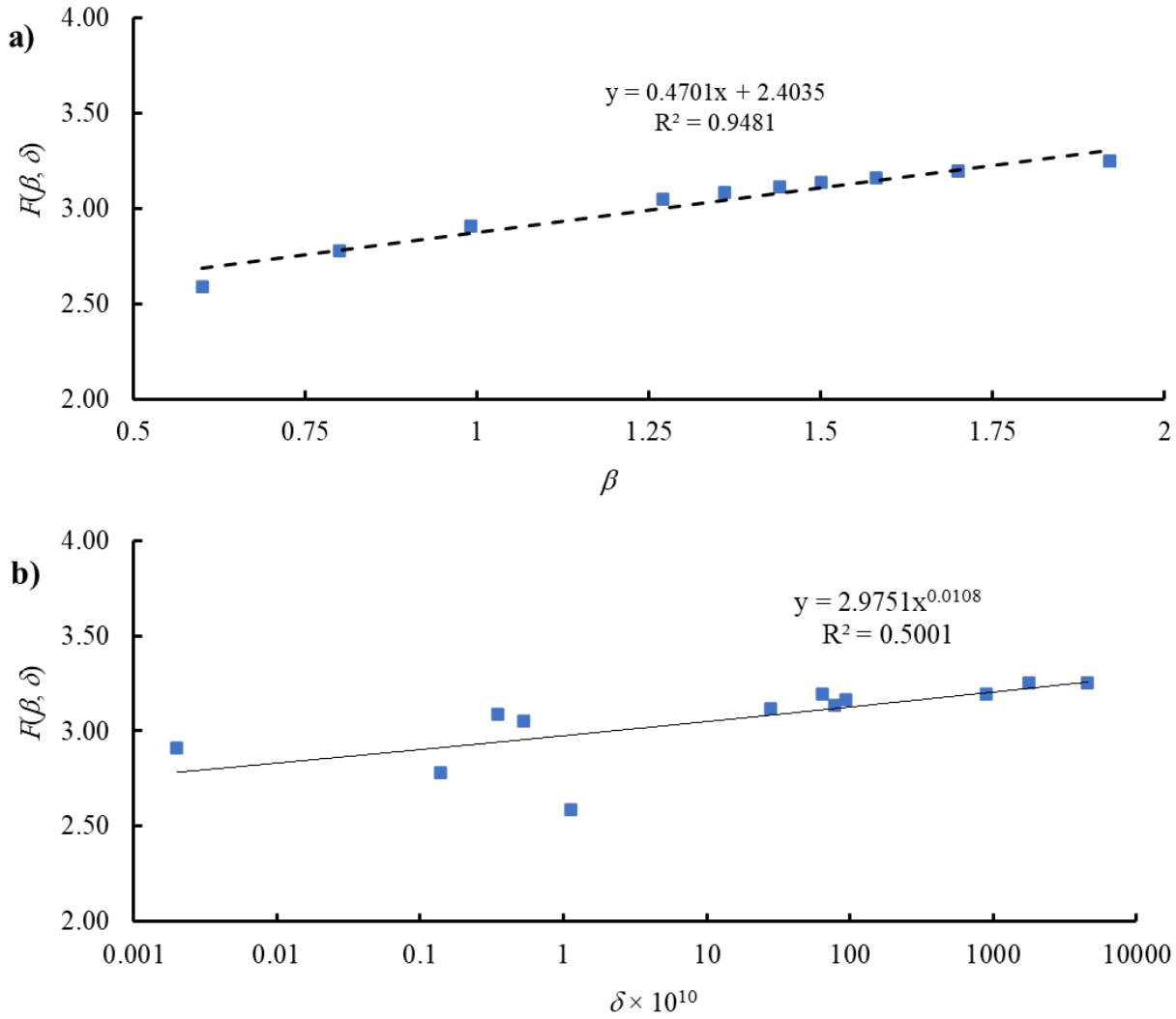

Figure 2- Variation in the functional relationship $F(\ ,\ )$ versus $\ $ (a) and $\ $ (b) for the twelve USDA soil textural classes. The $F(\ ,\ )$ values are computed for an initial water pressure head of 10000 cm.

$F(\ ,\ )$ vs. $F(\ )$

The effect of on t_{grav} was explored by comparing $F(\ ,\ )$ and $F(\ )$, with $F(\ )$ being equal to $F(\ ,\ )$ when is set to zero, i.e., $F(\ ) = F(\ ,\ = 0)$. Our analysis found a power function between $F(\ ,\ )$ and as shown in Fig. 2, with a very low values for the exponent, i.e., 0.0108. That shows that had a very small influence and that setting $= 0$ did not lead to any changes in the $F(\ ,\ )$ values and consequently also not in t_{grav}. By setting $= 0$ one will also obtain the same results for both cases as shown in Fig. 1, which may be a consequence of the values being very close to zero for all examined soil classes, except for clay and silty clay and to a lesser extent also silty clay loam (Fig. 3). It is also likely, that the power function found between $F(\ ,\ )$ and (Fig. 2) represents the indirect effects of on $F(\ ,\ )$ since a relationship exists between and the soil hydraulic parameters.

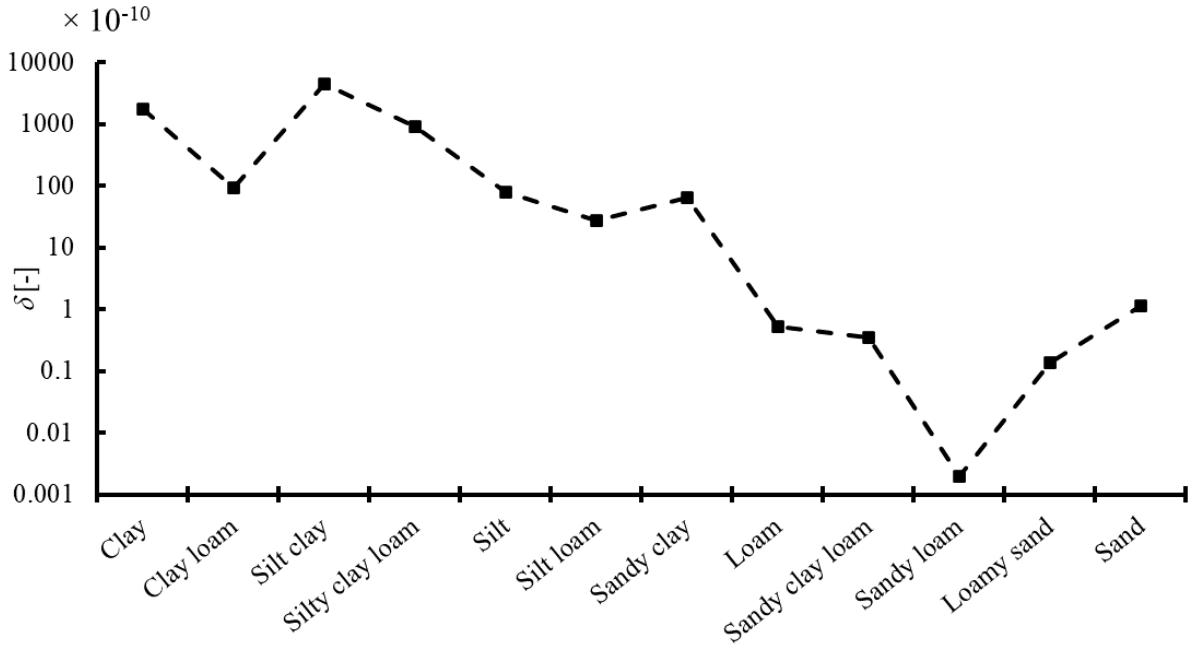

Figure 3- Variation in the functional coefficient among the twelve USDA soil textural classes. The values are obtained for an initial water pressure head of 10000 cm.

To examine this effect in more detail, the surface response function between and m and/or $S_{e,i}$ was explored (Fig. 4), whereby all parameters were allowed to vary within a physically meaningful range. MvG m values were allowed to vary between 0 and 0.7, the latter corresponding to the highest n value (here m = 1-1/n) among the studied soil classes. We note here that smaller m values generally correspond to more fine-textured soils involving broader pore-

and particle-size distributions, while higher m values correspond to more coarse textured soils. The value of $S_{e,i}$ was varied between 0 and 0.9, but without $S_{e,i}$ values higher than 0.9 since infiltration rates may be less when a soil initially is nearly saturated. As can be seen from Fig. 4, is close to zero for all soils when $S_{e,i}$ is less than 0.6. In the case of medium- and fine-textured soils (with m 0.4), is even close to zero over the complete range of $S_{e,i}$ values. Figure 4 therefore clearly indicates that will have considerable effect on $F(\ ,\ )$, and consequently on t_{grav}, only when infiltration will occur in coarse textured soils at a relatively high degree of saturation (e.g., $S_{e,i} > 0.7$) at the start of the infiltration process. The latter condition seldom occurs in nature since coarse-textured soils usually are drained fast after saturation. We are hence confident that ignoring in our formulation will not impact the overall predictions. Consequently, we use $F(\ ,\ =0)$ whenever the AAP solution for t_{grav} is used or discussed, and for simplicity use from here on only the term $F(\ )$ throughout the text.

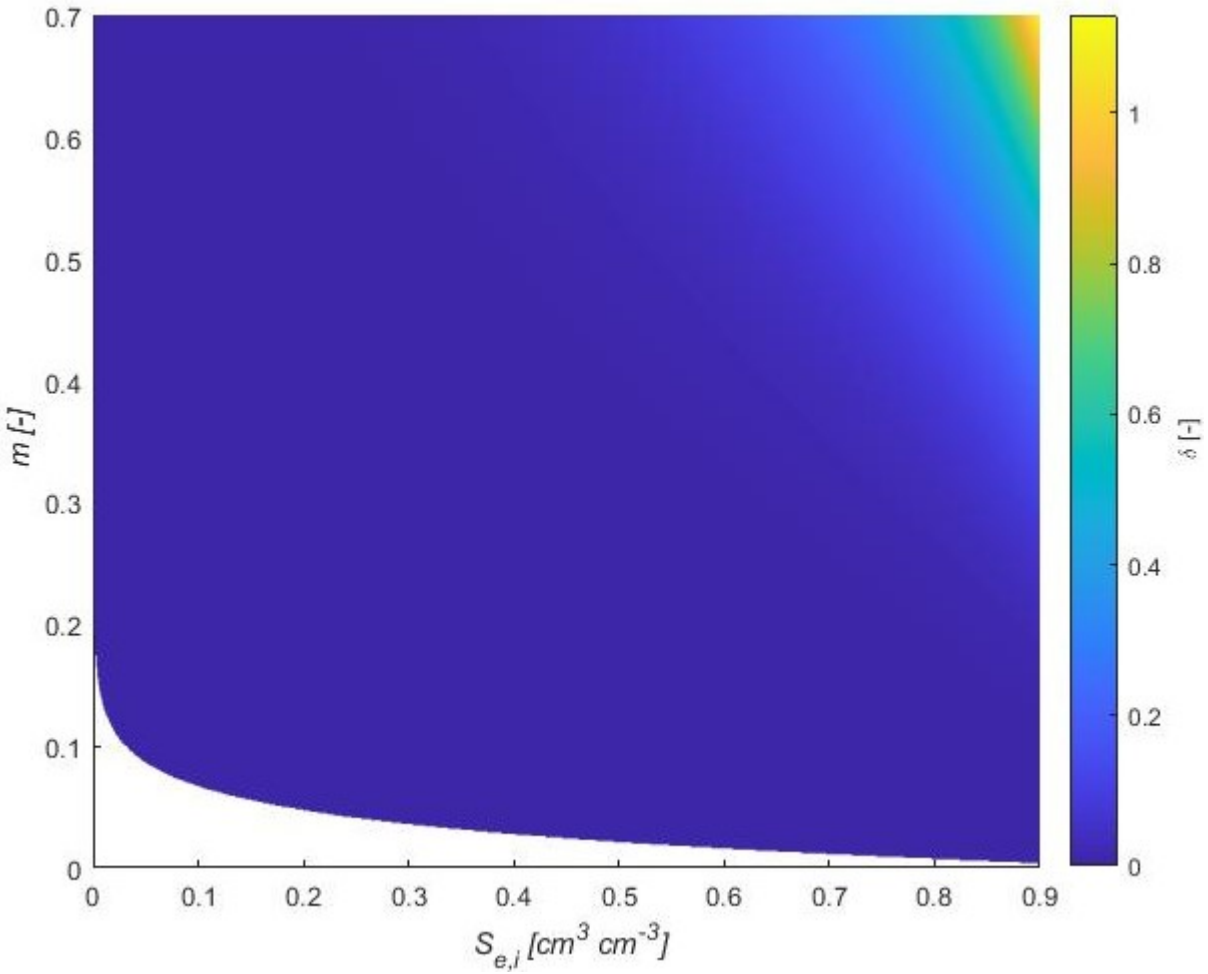

Figure 4- Surface response function for with respect to changes in the initial saturation degree of soils ($S_{e,i}$), and the parameter m in van Genuchten (1980) water retention model.

Implicit vs. explicit solutions of t_{grav}

Still needed is a verification that the much simpler explicit solutions given by Eq. (32) provide accurate approximations of the implicit solutions of t_{grav} as given by Eq. (22). Figure 5 shows variations in $F(\ )$ versus for the twelve soil textural classes when using AAP and the 3T, 4T and 5T expansions. In the case of 4T and 5T expansions, the $F(\ )$ is solved using the same methodology defined in Eq. (17). In the case of implicit solution of t_{grav}, $F(\ )$ was always higher than 2.6 for all textural classes, with $F(\ )$ linearly increasing with increasing . In contrast, a second-order polynomial trend between $F(\ )$ and is present when the 3T explicit solution is used, with a maximum of about 3.6 in $F(\ )$ when values were about 1.3, and lower $F(\ )$ elsewhere. A similar trend as for the implicit solution of t_{grav}, albeit with a smaller slope, existed between $F(\ )$ and when the 4T expansion was used. The 5T approximate expansion also showed a second-order polynomial trend between $F(\ )$ and , but less nonlinear and with mostly a negative slope.

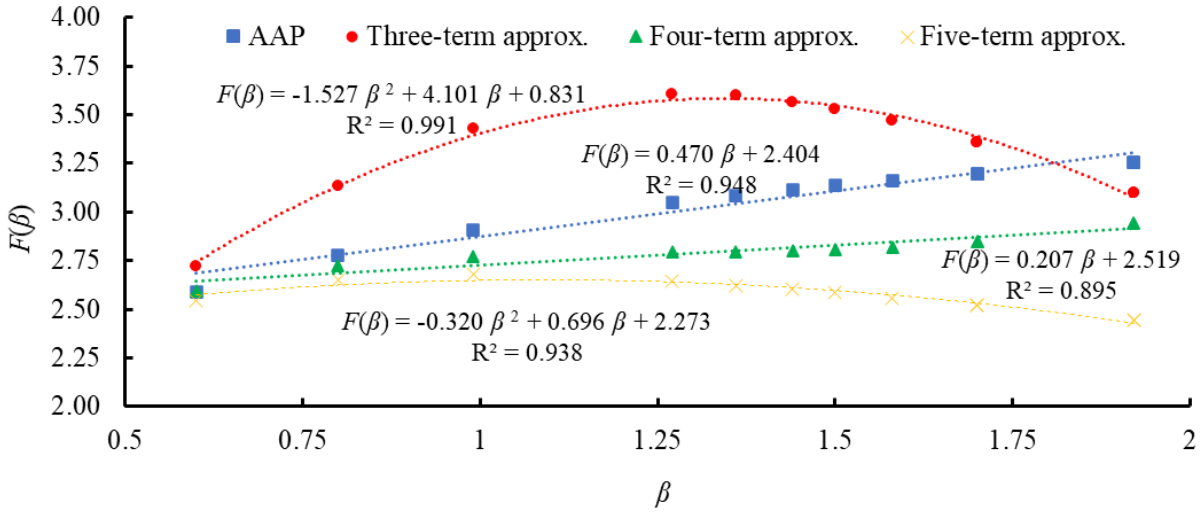

Figure 5- Variations in the function F( ) versus for the twelve USDA soil textural classes.

Figure 5 indicates that the approximate expansions are relatively far away from the implicit solution of t_{grav}, especially at long infiltration times, with the $F(\ )$ values showing that the reformulated equation for t_{grav} is 2.69 to 3.25 times larger than the classical t_{grav} model given by Eq. (3). We conclude that the expansions will never be valid for steady-state infiltration, regardless of the

number of terms considered. Since t_{grav} identifies the shift between the relative weights of capillary and gravity, the expansions may still be valid depending on their divergence. It is important to emphasize here that the expansions to approximate the AAP are only valid if $I \ll \frac{S^2}{(2K_s\beta)}$. Using more terms make the expansion hence more precise inside the range of validity, but this will not extend the range in terms of total infiltration amount or total time. Using the simplified equations outside of this range will generate large errors, and possibly even larger ones when including more terms in the approximation.

The above results indicate that precise calculations of t_{grav} require the use of Parlange's AAP solution. However, we explored this more directly comparing the obtained t_{grav} values from both implicit and explicit solutions. Figure 6 shows the expected differences in t_{grav} between the implicit and explicit solutions. We excluded the 4T and 5T expansions since they are more complicated to solve and still inaccurate compared to AAP implicit solution (especially for large values). We also excluded the silty clay soil textural class from presentation since it has a t_{grav} value of about 1000 h, about three orders of magnitude higher than most of the other soils leading to ambiguous results. The results plotted in Fig. 6 show that the differences between implicit and explicit solutions are very smaller than what expected from $F(\,)$ comparisons. To check the null hypothesis that the pairwise difference between data vectors has a mean equal to zero, a paired-sample t-Test at a probability of $p < 0.05$ was performed. The results indicates that the differences in the t_{grav} values are statistically insignificant. Therefore, given that the implicit solution is time-consuming and complicated, application of the explicit formulation is to be recommended for practical problems.

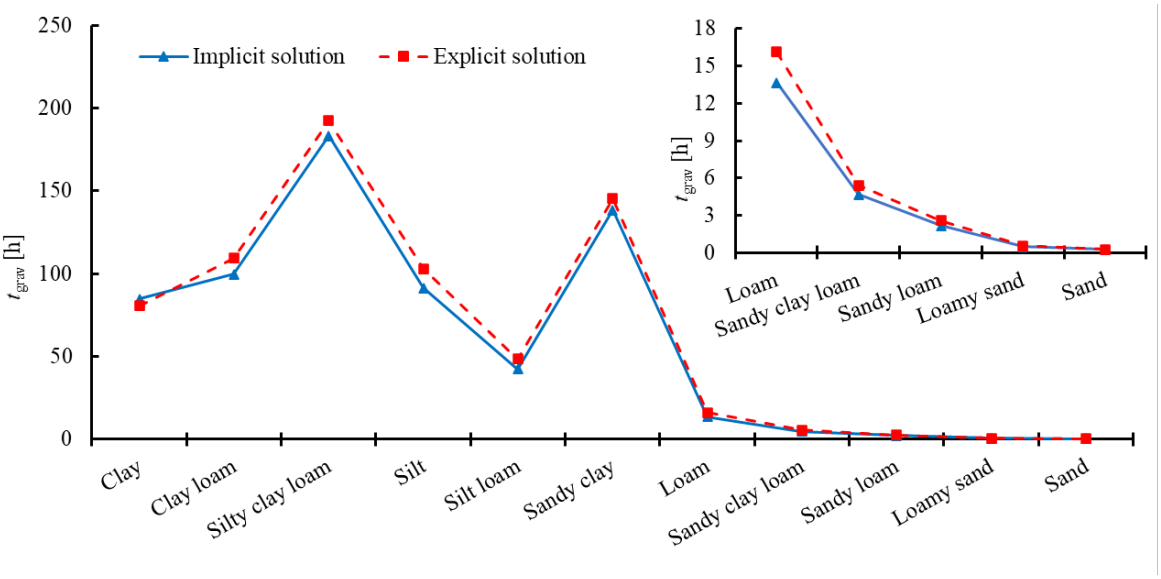

Figure 6- Variations in the soil characteristic time, t_{grav}, determined using the

implicit and explicit solutions (based on the three terms) of t_{grav} for the examined soil textural classes. Results for silty clay were not shown because of its extremely high t_{grav} value.

Influence of on t_{grav}

Given the fact that is very difficult to estimate and its value has little effect on 1D infiltration (e.g., Latorre et al., 2018; Rahmati et al., 2020), we analyzed the effect of on t_{grav} using a constant of 0.6 as suggested by Haverkamp et al. (1994) versus soil-dependent according to Eq. (7). In this section we limit ourselves to the explicit solution only since the implicit solution would give essentially the same results, as discussed in previous section (Fig. 6). As can be seen from Fig. 7, a constant value of 0.6 does not represent t_{grav} very well for the 12 USDA soil classes. A paired-sample t-Test at $p < 0.05$ showed that our null hypothesis that the pairwise difference between data vectors has a mean equal to zero is to be rejected, meaning that the differences between t_{grav} values are statistically significant for many of the soil textural classes. Assuming a constant of 0.6 seems to be applicable only for coarse-textured soils such as sand and loamy sand.

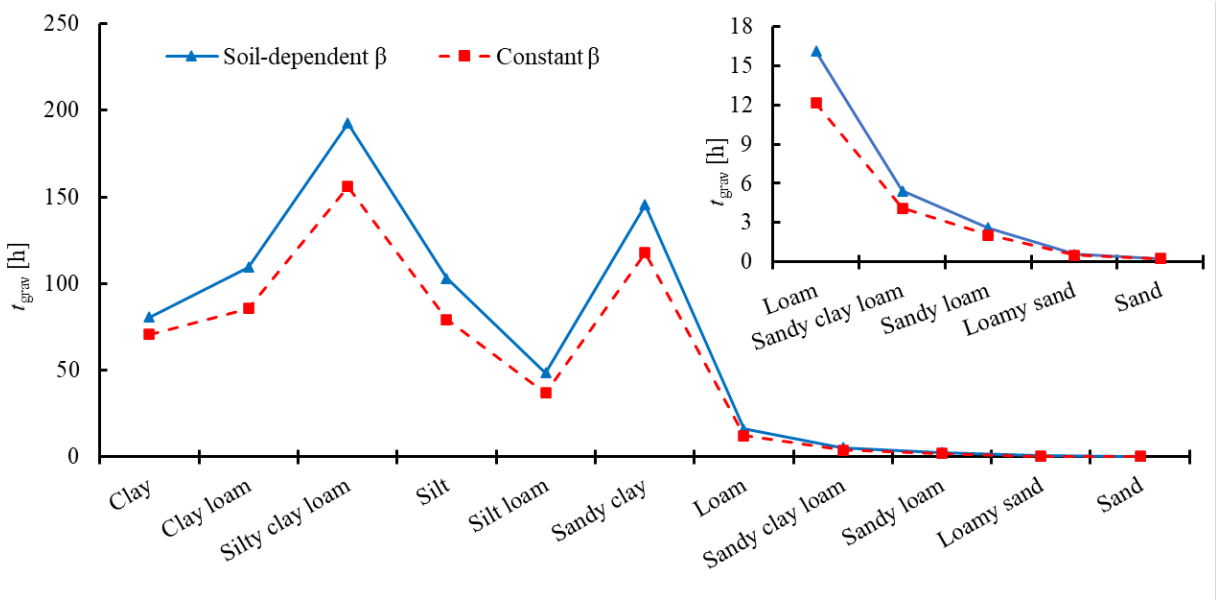

Figure 7- Soil characteristic times, t_{grav}, determined using the explicit solution assuming soil dependent values (Eq. 7) as well as a constant value of 0.6 as suggested by Haverkamp et al. (1994). Silty clay was excluded from the plot because of its unreasonably high t_{grav} value leading to misrepresentation of the chart. The inset shows differences between the two approaches for coarser soils.

Application of $t_{\mathbf{grav}}$

Many studies previously have used t_{grav} from different perspectives. Philip (1957) himself used the parameter (denoted here as $t_{\text{grav, Philip}}$) as a priory indicator to determine the convergence time of his TSE solution. We therefore briefly explored if t_{grav} and $t_{\text{grav, Philip}}$ accurately represented the convergence times of Philip's TSE solution and/or the approximate expansions by analyzing 1D simulated infiltration curves obtained with the HYDRUS-1D software. Results are shown in Fig. 8 for the 12 soil textural classes. Included in Fig. 8 is steady-state infiltration curves obtained with Haverkamp et al. (1994) long term equation where the 3D term is set to zero to fit the 1D infiltration as it was included for this purpose (see equation 4 in Haverkamp et al., 1994):

$$I_{\text{ssi}}(t) = K_s t + \frac{\ln\left(\frac{1}{\beta}\right) S^2}{2(K_s - K_i)(1-\beta)} \quad (33)$$

As can be seen from the results in Fig. 8, $t_{\text{grav, Philip}}$ was not a good convergence indicator for the HYDRUS-1D curves as well as all TSE approximations, being very late to determine a valid time domain for its safe use. Interestingly, Fig. 8 shows that in nearly all cases, Philip's 2T equation diverged from the simulated data already at small infiltration times, thus suggesting that his approach should be used with caution, especially for late infiltration times. The 3T equation serves represented infiltration well, even at later times when its curve started to diverge from the simulated HYDRUS-1D curves. The reformulated t_{grav} furthermore seemed to serve as a good indicator for the convergence time of the 3T equation.

Another interesting feature of Fig. 8 is that 4T and 5T approximate expansions produced infiltration rates which increasingly deviated from the simulated curves as well as the 3T solution. We discussed this before and then we prevent ourselves expending more on this.

Ross et al. (1996) previously used $t_{\text{grav, Philip}}$ and $I_{\text{grav, Philip}}$ to scale times ($t^* = \frac{2t}{t_{grav,\ \ Philip}}$) and cumulative infiltration rates ($I^* = \frac{2I}{I_{grav,\ \ Philip}}$) to obtain a dimensionless implicit analytical equation for infiltration. Their equation could be used to determine dimensionless parameters of the normalized soil water retention and hydraulic conductivity functions. Using re-formulated t_{grav} and I_{grav} values instead of $t_{\text{grav, Philip}}$ and $I_{\text{grav, Philip}}$ to scale the infiltration data would produce then different scaling factors and indirectly lead to different predictions of the hydraulic parameters. While beyond the scope of our current study, this topic should be analyzed in future research.

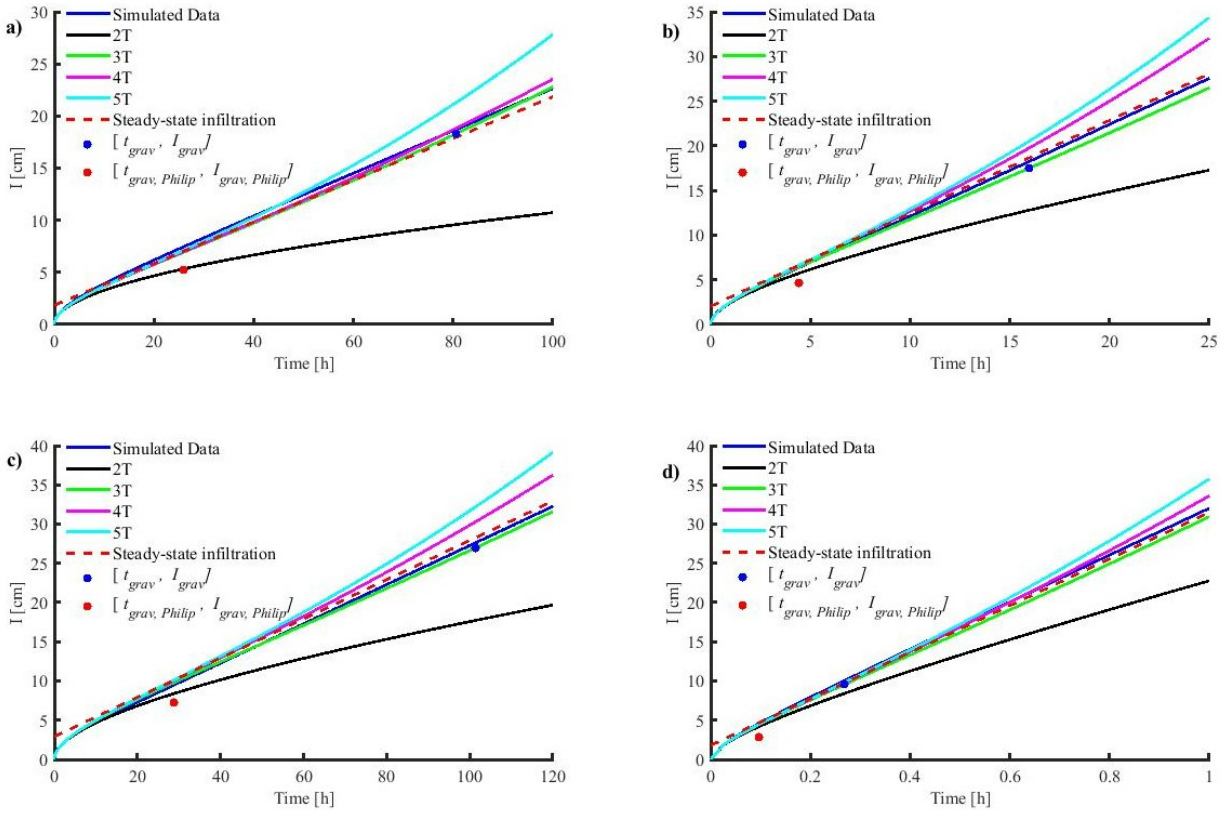

Figure 8- Simulated infiltration curves obtained with HYDRUS-1D and the approximate 2T, 3T 4T and 5T expansions as obtained for the 4 out of 12 USDA soil textural classes (a: clay, b: loam, c: silt, and d: sand). Also shown is the steady-state infiltration curve of Haverkamp et al. (1994) matched to the latest simulation data. The red and blue dots show the relationships between convergence time of Philip's time series expansion (TSE) and the reformulated t_{grav} and classical $t_{grav,\ Philip}$ characteristic times.

In a study comparing the accuracy of K_s data obtained using positive-head tension infiltrometer and single-ring pressure infiltrometer techniques relative to classical undisturbed soil core measurements, Reynolds et al. (2000) used $t_{grav,\ Philip}$ as an index of the time at which steady-state infiltration would be reached. We briefly evaluated if the reformulated t_{grav} or $t_{grav,\ Philip}$ represented the time to reach steady-state infiltration well. For this, we used the Haverkamp et al. (1994) steady-state infiltration equation (Eq. 33) first to calculate steady-state infiltration (I_{ssi}) for all of our test data. In a second step, a 1st order polynomial was fitted to the I_{ssi}-t data. Keeping the slope of the fitted polynomial unchanged, the intercept was recalibrated using the last datapoint of the calculated curve to ensure that the recalibrated steady-state line fitted the late

infiltration times well. Steady-state infiltration was assumed to be reached when the numerically simulated Hydrus-1D cumulative infiltration became identical to the recalibrated steady-state infiltration data based on Eq. (33). Results in Fig. 9 show that for coarse textured soils, $t_{grav,\ Philip}$ and t_{grav} both served as a good indicator to determine the time when steady-state infiltration is reached. However, t_{grav} of the fine-textured soils was too conservative (much to the right of the tangent departure point), whereas $t_{grav,\ Philip}$ often was located to the left indicating too early times for steady-state infiltration. It seems that some in between t_{grav} and $t_{grav,\ Philip}$ would capture the time to steady-state infiltration more accurately. In the case of intermediate soil textures (loam, silt, silty clay, and silty clay loam), both criteria seemed to fall beyond the time when steady-state is reached, and therefore, neither $t_{grav,\ Philip}$ nor t_{grav} would then be good measures to define the time when steady-state infiltration will be reached.

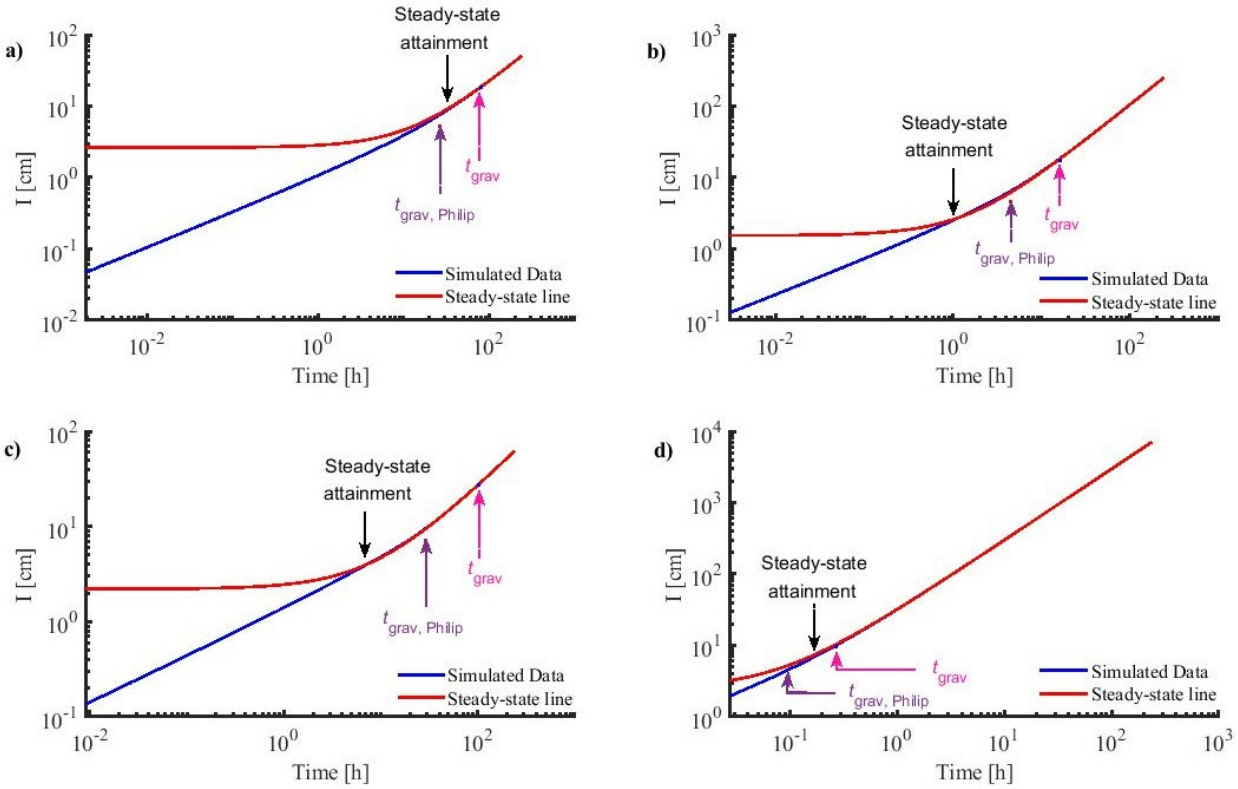

Figure 9- Relationships between the time to reach steady-state infiltration and the reformulated t_{grav} and classical $t_{grav,\ Philip}$ characteristic times for the 4 out of 12 USDA soil classes (a: clay, b: loam, c: silt, and d: sand). Simulated data were based on HYDRUS-1D simulations.

Using a Beerkan Estimation of Soil Transfer (BEST) method, Lassabatere et al. (2006) further used $t_{grav,\ Philip}$ to determine the maximum time, t_{max}, for which

transient expressions as well as the S and K_s predictions are considered valid. For this, they used the following equation $t_{max:}$

$$t_{\max} = \frac{1}{4(1-B)^2} t_{grav,\quad Philip} \tag{34}$$

where B is a constant. Considering that the reformulated t_{grav} improves the estimation of the maximum time, using it in the BEST method may result in different accuracies for the S and K_s predictions.

Rahmati et al. (2020) also showed that inferring soil hydraulic properties (S and K_s) from infiltration data works best when the infiltration data are measured until t_{grav} is reached, whereby t_{grav} was determined using similar concepts as in this paper. The authors furthermore showed that infiltration measurements for durations shorter than t_{grav} could lead to significant errors in the predictions, particularly when estimating K_s. Their results similarly indicate that infiltration measurement to be long enough for robust interpretations during practical measurement campaigns, especially for field studies.

Conclusions

Studying the infiltration process by which water enters the soil surface, nobody can ignore the seminal paper of Philip (1957) through which a time series expansion (TSE) for cumulative infiltration is provided. However, Philip (1957) has used gravity time, t_{grav}, to determine the convergence time of his TSE. He introduced t_{grav} to be a time when the effect of gravity on infiltration is expected to be as great as that of capillarity, and formulated this parameter in terms of sorptivity (S) as well as the saturated (K_s), and initial (K_i) hydraulic conductivities ($t_{grav,\ \text{Philip}} = \frac{S^2}{(K_s - K_i)^2}$) using the two first terms of his TSE. Regardless of whether t_{grav} serves as a good indicator for the convergence time of Philip's TSE and/or its approximate expansions, it is of great interest to reformulate t_{grav} using all possible terms of TSE or another general infiltration formulation which is valid for entire infiltration times. This because the higher order terms in the TSE are known to exert a significant impact on infiltration, with the truncated two-term equation of Philip failing to describe infiltration appropriately at especially longer times. On the other hand, theoretically, t_{grav} is a general concept being valid regardless of the infiltration model that is being used. For these reasons we reformulated t_{grav} to be $t_{grav} = F(\beta)\frac{S^2}{(K_s - K_i)^2}$ using the Analytic Approximation (AAP) of Parlange et al. (1982) which has no time constraints. Using AAP made it possible to explore the effects of the fourth parameter (a soil specific shape parameter) on t_{grav} in addition to S, K_s, and K_i. The effects of on t_{grav} are exerted in the form of a functional relationship $F(\ )$. We provided both implicit and explicit solutions for $F(\ )$ and then examined the effects of (both constant and soil-dependent) and initial soil moisture

conditions on $F(\ )$, and consequently on t_{grav}. Finally, we examined the use of the classical $t_{\mathrm{grav,\ Philip}}$ as well as reformulated t_{grav} on the plausibility of these two parameters to serve as convergence criteria for Philip's TSE approach and its approximate expansions, and as a criterion for determining the time when steady state infiltration is reached. We also discussed the possible accuracy of the inferred soil hydraulic properties when classical and reformulated t_{grav} definitions are considered. Based on the results, following conclusions can be drawn:

- The reformulated t_{grav} is 2.59 to 3.25 times ($\overline{F(\beta)} = 3.1$) larger than the classical t_{grav}. Difference between the classical and reformulated t_{grav} parameters seem to be much higher in the case of fine-textured soils.
- Practically, a linear relationship exists between $F(\ )$ and , with higher values leading to higher $F(\ )$ values.
- The initial soil moisture content did not cause any changes in $F(\ )$ and consequently also not in t_{grav}, thus showing that for nearly all soil saturation degrees and soil types, K_{i} can be set to zero with little or no effects on the results.
- Although the differences between the implicit and explicit solutions of $F(\ )$ were considerable, final calculations of t_{grav} showed statistically no significant differences. Since the implicit solution is time-consuming and complicated, the explicit formulation is hence recommended for practical applications.
- Usage of a constant value of 0.6 for as suggested by Haverkamp et al. (1994), resulted in erroneous t_{grav} values compared to soil dependent values. We therefore strongly suggest avoiding using the constant for practical implications.
- The reformulated t_{grav} appeared to be a better indicator for the convergence time of Philip's TSE and its 3T approximation compared to classical $t_{\mathrm{grav,\ Philip}}$.
- The reformulated and classical t_{grav} expressions were both found to be suitable for the time when steady state infiltration is reached in coarse-textured soils. However, both performed poorly when applied to fine-textured soils, for which the reformulated t_{grav} was too conservative and $t_{\mathrm{grav,\ Philip}}$ too short.
- The reformulated t_{grav} will lead to far more accurate predictions of the soil hydraulic parameters (particularly K_{s}) from infiltration data as compared to $t_{\mathrm{grav,\ Philip}}$.

References

Assouline, S., & Ben-Hur, A., (2006). Effects of rainfall intensity and slope gradient on the dynamics of interrill erosion during soil surface sealing. *Catena*, 66, 211-220. https://doi.org/10.1016/j.catena.2006.02.005.

Carsel, R.F., & Parrish, R.S., (1988). Developing Joint Probability-Distributions of Soil-Water Retention Characteristics. *Water Resources Research*, 24, 755-769. https://doi.org/10.1029/WR024i005p00755.

Fuentes, C., Haverkamp, R., & Parlange, J.Y., (1992). Parameter Constraints on Closed-Form Soilwater Relationships. *Journal of Hydrology*, 134, 117-142. https://doi.org/10.1016/0022-1694(92)90032-Q.

Garrote, L., & Bras, R.L., (1995). An Integrated Software Environment for Real-Time Use of a Distributed Hydrologic Model. *Journal of Hydrology*, 167, 307-326. https://doi.org/10.1016/0022-1694(94)02593-Z.

Haverkamp, R., Ross, P., Smettem, K., & Parlange, J., (1994). Three-dimensional analysis of infiltration from the disc infiltrometer: 2. Physically based infiltration equation. *Water Resources Research*, 30, 2931-2935. https://doi.org/10.1029/94WR01788.

Iverson, R.M., (2000). Landslide triggering by rain infiltration. *Water resources research*, 36, 1897-1910. https://doi.org/10.1029/2000WR900090.

Kim, D., Ray, R.L., & Choi, M., (2017). Simulations of energy balance components at snow-dominated montane watershed by land surface models. *Environmental Earth Sciences*, 76, 337. https://doi.org/10.1007/s12665-017-6655-0.

Kutílek, M., & Krejca, M., (1987). Three-parameter infiltration equation of Philip type. *Vodohosp. cas*, 35, 52-61.

Lassabatere, L., Angulo-Jaramillo, R., Soria-Ugalde, J.M., Simunek, J., & Haverkamp, R., (2009). Numerical evaluation of a set of analytical infiltration equations. *Water Resources Research*, 45. https://doi.org/10.1029/2009wr007941.

Lassabatere, L., Angulo-Jaramillo, R., Ugalde, J.M.S., Cuenca, R., Braud, I., & Haverkamp, R., (2006). Beerkan estimation of soil transfer parameters through infiltration experiments - BEST. *Soil Science Society of America Journal*, 70, 521-532. https://doi.org/10.2136/sssaj2005.0026.

Latorre, B., Moret-Fernández, D., Lassabatere, L., Rahmati, M., López, M., Angulo-Jaramillo, R., Sorando, R., Comín, F., & Jiménez, J., (2018). Influence of the parameter of the Haverkamp model on the transient soil water infiltration curve. *Journal of Hydrology*, 564, 222-229. https://doi.org/10.1016/j.jhydrol.2018.07.006.

Lehmann, P., & Or, D., (2012). Hydromechanical triggering of landslides: From progressive local failures to mass release. *Water Resources Research*, 48. https:

//doi.org/10.1029/2011wr010947.

MacDonald, M.K., Pomeroy, J.W., & Essery, R.L.H., (2018). Water and energy fluxes over northern prairies as affected by chinook winds and winter precipitation. *Agricultural and Forest Meteorology*, 248, 372-385. https://doi.org/10.1016/j.agrformet.2017.10.025.

Moret-Fernández, D., Latorre, B., López, M.V., Pueyo, Y., Lassabatere, L., Angulo-Jaramilo, R., Rahmati, M., Tormo, J., & Nicolau, J.M., (2020). Three-and four-term approximate expansions of the Haverkamp formulation to estimate soil hydraulic properties from disc infiltrometer measurements. *Hydrological Processes*, 34, 5543-5556. https://doi.org/10.1002/hyp.13966.

Mualem, Y., (1976). A new model for predicting the hydraulic conductivity of unsaturated porous media. *Water resources research*, 12, 513-522. https://doi.org/10.1029/WR012i003p00513.

Parlange, J.-Y., Lisle, I., Braddock, R., & Smith, R., (1982). The three-parameter infiltration equation. *Soil Science*, 133, 337-341. https://doi.org/10.1097/00010694-198206000-00001.

Philip, J., (1957). The theory of infiltration: 1. The infiltration equation and its solution. *Soil science*, 83, 345-358. http://dx.doi.org/10.1097/00010694-195705000-00002.

Philip, J., & Farrell, D., (1964). General solution of the infiltration-advance problem in irrigation hydraulics. *Journal of Geophysical research*, 69, 621-631. https://doi.org/10.1029/jz069i004p00621.

Poesen, J., & Valentin, C., (2003). Gully erosion and global change - Preface. *Catena*, 50, 87-89. https://doi.org/10.1016/S0341-8162(02)00146-7.

Rahmati, M., Latorre, B., Lassabatere, L., Angulo-Jaramillo, R., & Moret-Fernandez, D., (2019). The relevance of Philip theory to Haverkamp quasi-exact implicit analytical formulation and its uses to predict soil hydraulic properties. *Journal of Hydrology*, 570, 816-826. https://doi.org/10.1016/j.jhydrol.2019.01.038.

Rahmati, M., Rezaei, M., Lassabatere, L., Morbidelli, R., & Vereecken, H., (2021). Simplified characteristic time method for accurate estimation of the soil hydraulic parameters from one-dimensional infiltration experiments. *Vadose Zone Journal*, 20, e20117. https://doi.org/10.1002/vzj2.20117.

Rahmati, M., Vanderborght, J., Simunek, J., Vrugt, J.A., Moret-Fernandez, D., Latorre, B., Lassabatere, L., & Vereecken, H., (2020). Soil hydraulic properties estimation from one-dimensional infiltration experiments using characteristic time concept. *Vadose Zone Journal*, 19, e20068. https://doi.org/10.1002/vzj2.20068.

Reynolds, W.D., Bowman, B.T., Brunke, R.R., Drury, C.F., & Tan, C.S., (2000). Comparison of tension infiltrometer, pressure infiltrometer, and soil core esti-

mates of saturated hydraulic conductivity. *Soil Science Society of America Journal*, 64, 478-484. https://doi.org/10.2136/sssaj2000.642478x.

Richards, L.A., (1931). Capillary conduction of liquids through porous mediums. *Physics-a Journal of General and Applied Physics*, 1, 318-333. https://doi.org/10.1063/1.1745010.

Ross, P.J., Haverkamp, R., & Parlange, J.Y., (1996). Calculating parameters for infiltration equations from soil hydraulic functions. *Transport in Porous Media*, 24, 315-339. https://doi.org/10.1007/Bf00154096.

Šimůnek, J., Genuchten, M.T., & Šejna, M., (2008). Development and Applications of the HYDRUS and STANMOD Software Packages and Related Codes. *Vadose Zone Journal*, 7, 587-600. https://doi.org/10.2136/vzj2007.0077.

Šimůnek, J., Van Genuchten, M.T., & Šejna, M., (2016). Recent developments and applications of the HYDRUS computer software packages. *Vadose Zone Journal*, 15, vzj2016. 2004.0033. https://doi.org/10.2136/vzj2016.04.0033.

van Genuchten, M.T., (1980). A closed-form equation for predicting the hydraulic conductivity of unsaturated soils. *Soil science society of America journal*, 44, 892-898. https://doi.org/10.2136/SSSAJ1980.03615995004400050002X.

Varado, N., Braud, I., Ross, P.J., & Haverkamp, R., (2006). Assessment of an efficient numerical solution of the 1D Richards' equation on bare soil. *Journal of Hydrology*, 323, 244-257. https://doi.org/10.1016/j.jhydrol.2005.07.052.

Vereecken, H., Weihermuller, L., Assouline, S., Simunek, J., Verhoef, A., Herbst, M., Archer, N., Mohanty, B., Montzka, C., Vanderborght, J., Balsamo, G., Bechtold, M., Boone, A., Chadburn, S., Cuntz, M., Decharme, B., Ducharne, A., Ek, M., Garrigues, S., Goergen, K., Ingwersen, J., Kollet, S., Lawrence, D.M., Li, Q., Or, D., Swenson, S., de Vrese, P., Walko, R., Wu, Y.H., & Xue, Y.K., (2019). Infiltration from the Pedon to Global Grid Scales: An Overview and Outlook for Land Surface Modeling. *Vadose Zone Journal*, 18. https://doi.org/10.2136/vzj2018.10.0191.

Verhoef, A., & Egea, G., (2013). Soil water and its management, In: Peter J., G., & Stephen, N. (Eds.), *Soil conditions and plant growth*, pp. 269-322. https://doi.org/10.1002/9781118337295.ch9.

Waechter, R., & Philip, J., (1985). Steady two-and three-dimensional flows in unsaturated soil: The scattering analog. *Water Resources Research*, 21, 1875-1887. https://doi.org/10.1029/WR021i012p01875.

Figures Captions:

Figure 1. Variation in the functional relationship F(,) and reformulated and classical characteristic times (t_{grav} [h]) for the twelve USDA soil textural classes. Note that soils are ranked based on their texture and no function is defined for them.

Figure 2- Variation in the functional relationship F(,) versus (a) and (b) for the twelve USDA soil textural classes. The F(,) values are computed for an initial water pressure head of 10000 cm.

Figure 3- Variation in the functional coefficient among the twelve USDA soil textural classes. The values are obtained for an initial water pressure head of 10000 cm.

Figure 4- Surface response function for with respect to changes in the initial saturation degree of soils ($S_{e,i}$), and the parameter m in van Genuchten (1980) water retention model.

Figure 5- Variations in the function F( ) versus for the twelve USDA soil textural classes.

Figure 6- Variations in the soil characteristic time, t_{grav}, determined using the implicit and explicit solutions (based on the three terms) of t_{grav} for the examined soil textural classes. Results for silty clay were not shown because of its extremely high t_{grav} value.

Figure 7- Soil characteristic times, t_{grav}, determined using the explicit solution assuming soil dependent values (Eq. 7) as well as a constant value of 0.6 as suggested by Haverkamp et al. (1994). Silty clay was excluded from the plot because of its unreasonably high t_{grav} value leading to misrepresentation of the chart. The inset shows differences between the two approaches for coarser soils.

Figure 8- Simulated infiltration curves obtained with HYDRUS-1D and the approximate 2T, 3T 4T and 5T expansions as obtained for the 4 out of 12 USDA soil textural classes (a: clay, b: loam, c: silt, and d: sand). Also shown is the steady-state infiltration curve of Haverkamp et al. (1994) matched to the latest simulation data. The red and blue dots show the relationships between convergence time of Philip's time series expansion (TSE) and the reformulated t_{grav} and classical $t_{grav,\ Philip}$ characteristic times.

Figure 9- Relationships between the time to reach steady-state infiltration and the reformulated t_{grav} and classical $t_{grav,\ Philip}$ characteristic times for the 4 out of 12 USDA soil classes (a: clay, b: loam, c: silt, and d: sand). Simulated data were based on HYDRUS-1D simulations.